# Supporting Information: Nature of the "Z"-phase in Layered Na-ion Battery Cathodes

James W. Somerville,[a] Adam Sobkowiak,[a‡] Nuria Tapia-Ruiz,[a‡] Juliette Billaud,[b] Juan G. Lozano,[a‡] Robert A. House,[a] Leighanne C. Gallington,[c] Tore Ericsson,[d] Lennart Häggström,[d] Matthew R. Roberts,[a] Urmimala Maitra,[a‡] and Peter G. Bruce*[ae]

[a] Dept. of Materials, University of Oxford, Parks Road, Oxford OX1 3PH, UK

[b] Paul Scherrer Institut, Electrochemical Laboratory, CH-5232 Villigen PSI, CH

[c] X-ray Science Division, Advanced Photon Source, Argonne National Lab., Argonne, IL, USA

[d] Dept. of Chemistry, Ångstrom Lab., Uppsala University, Box 538, SE-751 21 Uppsala, SE

[e] The Faraday Institution, Quad One, Becquerel Avenue, Harwell Campus, Didcot, OX11 0RA, UK

* Corresponding Author: peter.bruce@materials.ox.ac.uk

**Inductively Coupled Plasma-Optical Emission Spectrometry**

ICP-OES was conducted on a PerkinElmer Optima 8000 ICP-OES.

Table S1: ICP-OES Composition Validation

| **Targeted Composition** | **Na** | **Ni** | **Mn** | **Fe** |
|---|---|---|---|---|
| $Na_{0.67}[Ni_{0.33}Mn_{0.67}]O_2$ | 0.70(2) | 0.32(1) | 0.68(1) | — |
| $Na_{0.67}[Ni_{0.25}Mn_{058}Fe_{0.17}]O_2$ | 0.68(2) | 0.23(1) | 0.60(3) | 0.18(1) |
| $Na_{0.67}[Ni_{0.17}Mn_{0.50}Fe_{0.33}]O_2$ | 0.67(3) | 0.153(4) | 0.53(2) | 0.32(2) |

**Constraints for Rietveld Refinements**

- Isotropic displacement values (Uiso) of sodium sites were constrained to be equivalent.
- Site occupancy fractions (SOF) of sodium sites were constrained to sum to the nominal stoichiometric value (e.g. 2/3 per formula unit for pristine).
- The SOF values for transition metals were fixed at the nominal stoichiometric values.
- The SOF values for oxygen were fixed at the nominal stoichiometric value.

**Rietveld Refinements of Synchrotron XRD Data**

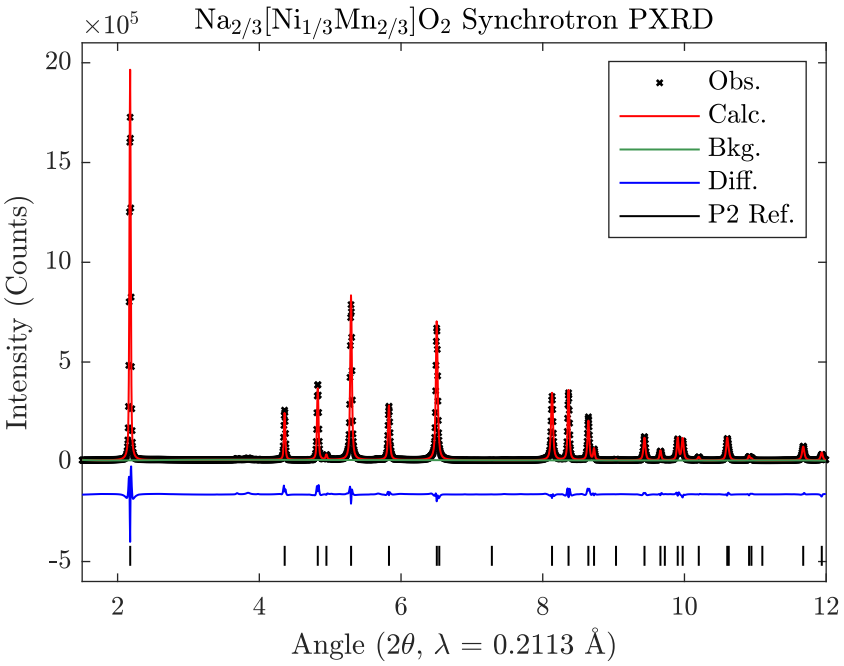


Figure S1: Rietveld refinement fitting of pristine $Na_{2/3}[Ni_{1/3}Mn_{2/3}]O_2$ from PXRD data collected at APS 11-ID-B with a wavelength of $\lambda = 0.2113$ Å.

Table S2: Rietveld refinement results for $Na_{2/3}[Ni_{1/3}Mn_{2/3}]O_2$.

| **SG: $P6_3/mmc$, *a*: 2.8968(1) Å, *c*: 11.1099(4) Å, V: 80.739(5) Å$^3$, Rexp: 0.58%, Rwp: 11.48%** | | | | | |
|---|---|---|---|---|---|
| **Atom** | **x** | **y** | **z** | **SOF** | **Uiso (Å$^2$)** |
| Na (2b) | 0 | 0 | 1/4 | 0.218(4) | 0.032(2) |
| Na (2d) | 2/3 | 1/3 | 1/4 | 0.449(4) | 0.032(2) |
| Ni (2a) | 0 | 0 | 0 | 1/3 | 0.0035(4) |
| Mn (2a) | 0 | 0 | 0 | 2/3 | 0.0035(4) |
| O (4f) | 2/3 | 1/3 | -0.0929(3) | 1 | 0.014(1) |

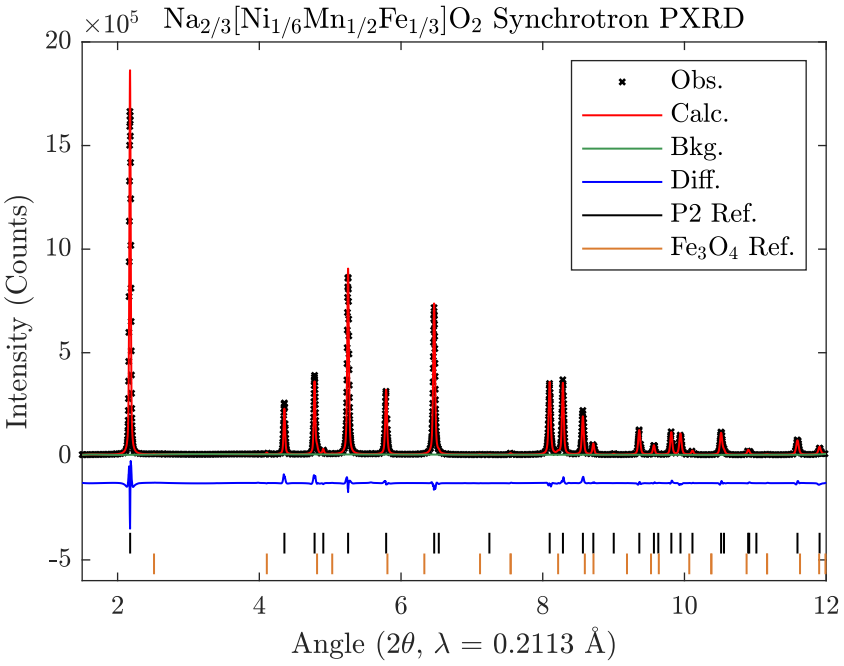


Figure S2: Rietveld refinement fitting of pristine $Na_{2/3}[Ni_{1/6}Mn_{1/2}Fe_{1/3}]O_2$ from PXRD data collected at APS 11-ID-B with a wavelength of $\lambda = 0.2113$ Å.

Table S3: Rietveld refinement results for $Na_{2/3}[Ni_{1/6}Mn_{1/2}Fe_{1/3}]O_2$ (98.5(3) wt.%).

| **SG: $P6_3/mmc$, *a*: 2.92527(4) Å, *c*: 11.1251(1) Å, V: 82.445(1) Å$^3$, Rexp: 0.58%, Rwp: 8.71%** | | | | | |
|---|---|---|---|---|---|
| **Atom** | **x** | **y** | **z** | **SOF** | **Uiso (Å$^2$)** |
| Na (2b) | 0 | 0 | 1/4 | 0.196(2) | 0.024(1) |
| Na (2d) | 2/3 | 1/3 | 1/4 | 0.471(2) | 0.024(1) |
| Ni (2a) | 0 | 0 | 0 | 1/6 | 0.0048(2) |
| Mn (2a) | 0 | 0 | 0 | 1/2 | 0.0048(2) |
| Fe (2a) | 0 | 0 | 0 | 1/3 | 0.0048(2) |
| O (4f) | 2/3 | 1/3 | -0.0940(1) | 1 | 0.0150(5) |

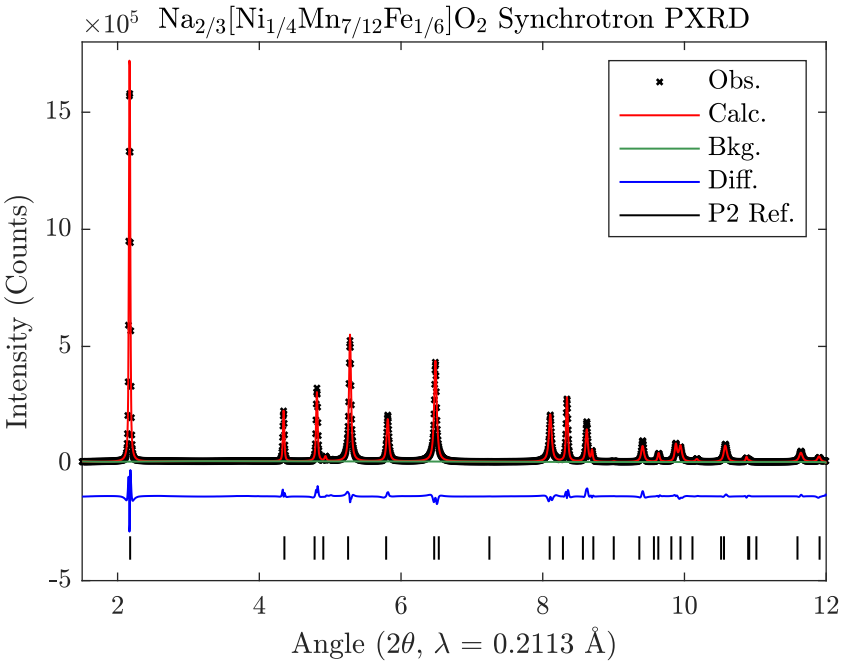


Figure S3: Rietveld refinement fitting of pristine $Na_{2/3}[Ni_{1/4}Mn_{7/12}Fe_{1/6}]O_2$ from PXRD data collected at APS 11-ID-B with a wavelength of $\lambda = 0.2113$ Å.

Table S4: Rietveld refinement results for $Na_{2/3}[Ni_{1/4}Mn_{7/12}Fe_{1/6}]O_2$.

| **S.G. *P6$_3$/mmc*, *a*: 2.9045(1) Å, *c*: 11.1467(5) Å, V: 81.434 (7) Å$^3$, Rwp: 11.41%, Rexp: 0.61%** | | | | | |
|---|---|---|---|---|---|
| **Atom** | **x** | **y** | **z** | **SOF** | **Uiso (*Å*$^2$)** |
| Na (2b) | 0 | 0 | 1/4 | 0.227(4) | 0.035(2) |
| Na (2d) | 2/3 | 1/3 | 1/4 | 0.440(4) | 0.035(2) |
| Ni (2a) | 0 | 0 | 0 | 1/4 | 0.0041(4) |
| Mn (2a) | 0 | 0 | 0 | 7/12 | 0.0041(4) |
| Fe (2a) | 0 | 0 | 0 | 1/6 | 0.0041(4) |
| O (4f) | 2/3 | 1/3 | -0.0910(3) | 1 | 0.011(1) |

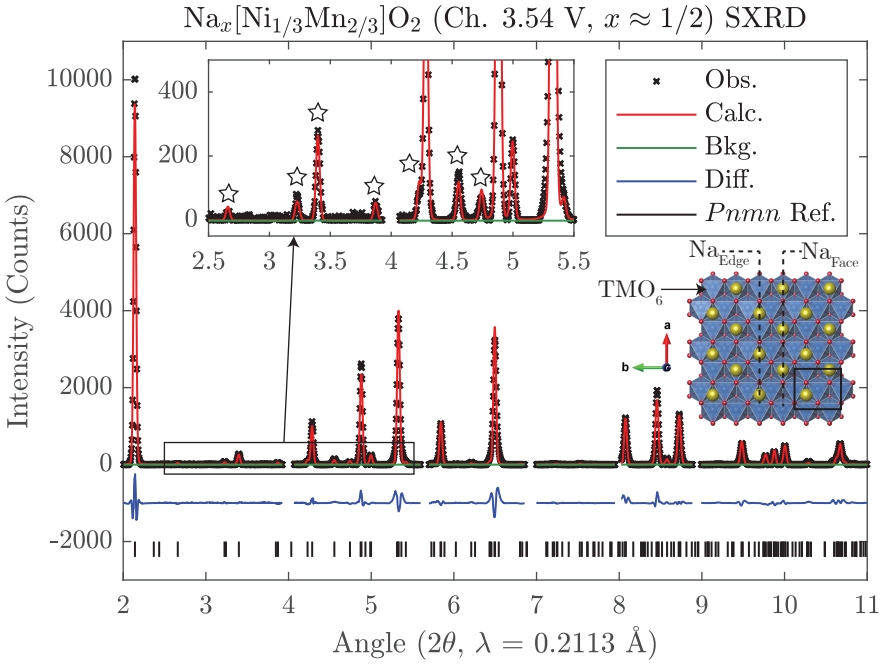


Figure S4: Rietveld refinement of $Na_x[Ni_{1/3}Mn_{2/3}]O_2$ ($x \approx 1/2$) from XRD data collected at APS 11-ID-B with a wavelength of $\lambda = 0.2113$ Å using the AMPIX cell. The material was charged to 3.54 V vs. $Na^+/Na$ in the cell and measured in *operando*-mode at this voltage. The data was reduced using GSAS-II, background subtracted using MATLAB, and then refined. Peaks from the Na metal counter electrode were excluded from the refinement. The inset shows the good fit of the low intensity peaks stemming from Na-ion ordering (marked with a star). This Na-ion ordering arrangement is equivalent to that of $Na_{1/2}CoO_2$, investigated by Huang et al.[1]

Table S5: $Na_x[Ni_{1/3}Mn_{2/3}]O_2$ (Ch 3.54 V) refined model parameters.

| **S.G. *Pnmn*, *a*: 4.9706(5) Å, *b*: 5.7229(4), *c*: 11.298(1) Å, V: 321.38(6) Å$^3$, Rwp: 23.71%, Rexp: 7.65%** | | | | | |
|---|---|---|---|---|---|
| **Atom** | **x** | **y** | **z** | **SOF** | **Uiso (*Å*$^2$)** |
| Na (2b) | -0.035(5) | 1/4 | 3/4 | 1 | 0.065(5) |
| Na (2a) | 0.331(5) | 3/4 | 3/4 | 1 | 0.065(5) |
| Ni (4e) | 0 | 1/4 | 0 | 0.013(1) | 1/3 |
| Mn (4e) | 0 | 1/4 | 0 | 0.013(1) | 2/3 |
| Ni (4d) | 1/2 | 0 | 0 | 0.013(1) | 1/3 |
| Mn (4d) | 1/2 | 0 | 0 | 0.013(1) | 2/3 |
| O (4e) | 0.322(2) | 1/4 | 0.103(2) | 0.035(3) | 1 |
| O (4e) | 0.347(4) | 3/4 | 0.067(2) | 0.035(3) | 1 |
| O (8g) | -0.172(2) | -0.012(2) | 0.083(1) | 0.035(3) | 1 |

## *Operando* XRD and Simulations

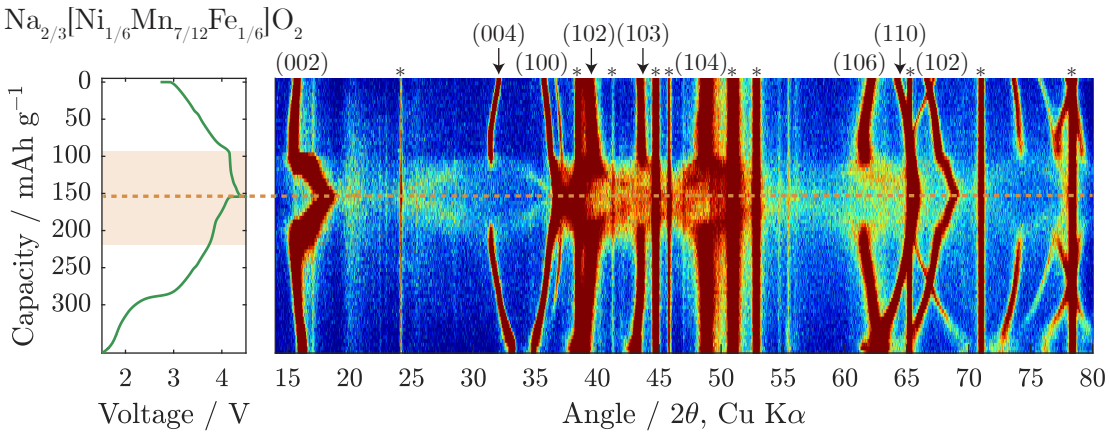


Figure S5: *Operando* XRD data are shown as a colourmap for $Na_{2/3}[Ni_{1/4}Mn_{7/12}Fe_{1/6}]O_2$. The top of charge is denoted by the orange dashed line and the region of electrochemical load curve corresponding to the "Z"-phase evolution is shaded orange.

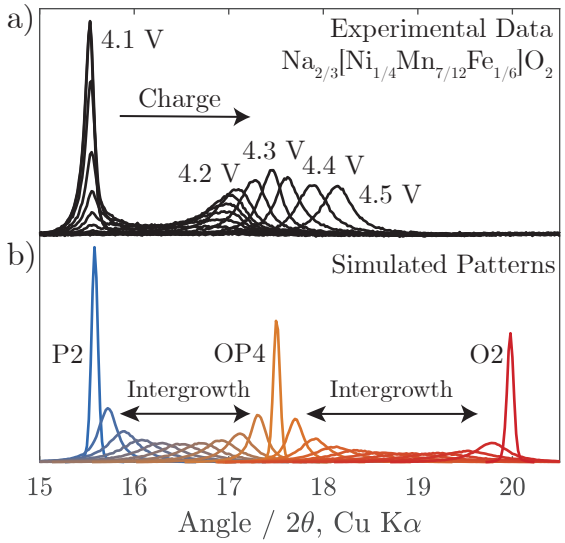


Figure S6: Comparison of operando XRD data of $Na_{2/3}[Ni_{1/4}Mn_{7/12}Fe_{1/6}]O_2$ with PXRD data simulated using FAULTS software as explained in the main text.

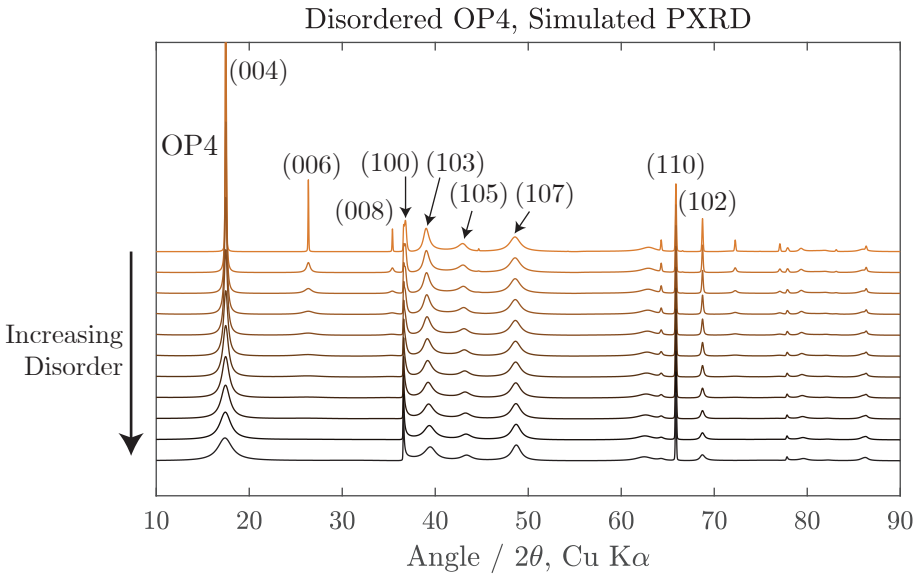


Figure S7: XRD patterns were simulated (using FAULTS) for the OP4 structure with varying amounts of disorder in the alternation of P and O-type layers. The top pattern simulates a perfectly ordered structure and the patterns below increase in disorder until a 100% disordered pattern is reached at the bottom.

# References

[1] Q. Huang, M. L. Foo, J. W. Lynn, H. W. Zandbergen, G. Lawes, Y. Wang, B. H. Toby, A. P. Ramirez, N. P. Ong and R. J. Cava, *Journal of Physics: Condensed Matter*, 2004, **16**, 5803–5814.